

# One-part geopolymer mixes from geothermal silica and sodium aluminate

Ailar Hajimohammadi\*, John L. Provis, and Jannie S.J. van Deventer

*Department of Chemical and Biomolecular Engineering*

*University of Melbourne, Victoria 3010, Australia*

*\* a.hajimohammadi@pgrad.unimelb.edu.au*

## Abstract

*At present, the most commonly used building material is ordinary Portland cement (OPC). However, OPC has a negative environmental effect during synthesis, with the release of significant amount of CO<sub>2</sub> greenhouse gas. The cement industry is responsible for 5-8% of total global anthropogenic CO<sub>2</sub> emissions. Geopolymerization is a technology capable of turning industrial wastes into strong and chemically durable cement-like binders, with significant Greenhouse emission savings. The synthesis of geopolymers can start from a variety of aluminosilicate sources such as fly ash or metakaolin. In geopolymer technology, alkali silicate solutions are frequently used to dissolve the solid aluminosilicate precursor to produce the binder. Sodium aluminate solutions have also been used. These corrosive and often viscous solutions are not user friendly, and would be difficult to use for bulk production. Developing geopolymers as a 1-part mixture (“just add water”) similar to OPC increases their commercial viability. Here, the geopolymer system consisting of geothermal silica and solid sodium aluminate (providing the solid silica, alkali and alumina sources), activated by addition of water, is studied. The effects of water content, high early silica and high early alumina in the formation of one part mix geopolymers are also investigated. XRD shows that the formulation with less water has an unexpected greater extent of crystallinity. It is also observed that a high early Al concentration inhibits geopolymerization, while a high early Si concentration enhances the reaction*

## 1. INTRODUCTION

The geopolymer structure is mainly an aluminosilicate gel network, where the silica gel structure is partially substituted with tetrahedral Al<sup>3+</sup> sites charge-balanced by alkali cations. The first stage of geopolymerization is the release of aluminate and silicate species from a solid source, which is usually achieved by alkali attack on an aluminosilicate material. First, the surface of the solid contacts the activating solution, and hydrolysis reactions begin to occur, later accompanied with the formation of oligomers and finally polycondensation of the oligomers to form a three-dimensional aluminosilicate network.[1] Soluble silicates are frequently used in geopolymer production for helping dissolution of the aluminosilicate starting material and governing the mechanical properties of the binder such as its compressive strength [2, 3]. In the present work, a solid silicate material and sodium aluminate are used as potential silica and

alumina replacements in the production of aluminosilicate cementitious binders.

The solid silicate material used in the current work is geothermal silica. The production of geothermal power results in large quantities of residual silica, frequently removed as scale build up in pipes [4]. At the Cerro Prieto geothermal plant in Baja California, Mexico, approximately 5 tonnes of silica per month is removed from process pipes and discarded to an evaporation lake [5]. This waste residue is a source of solid amorphous silica, which can potentially be used as a replacement for soluble silicate solution in geopolymerization.

## 2. EXPERIMENTAL PROCEDURE

Raw silica waste from the Cerro Prieto plant was washed with distilled water to remove salts and dried before use. The purified geothermal silica is 96% SiO<sub>2</sub> and contains small amounts of various salts. The silica particles should have a high enough surface area for reaction, but not so high as to compromise workability of the geopolymer paste. Geothermal silica has a very small fundamental particle size; however the particles are aggregated. [6]

Geothermal silica was mixed with solid sodium aluminate to attain Si/Al molar ratios of 1.5:1, 2:1 and 2.5:1, then water was added to these solid mixtures to attain samples with effective H<sub>2</sub>O/Na<sub>2</sub>O molar ratios of 7:1 and 12:1. The samples are named by these two ratios. The number outside parentheses refers to the Si/Al molar ratio and the number in the parentheses is the H<sub>2</sub>O/Na<sub>2</sub>O molar ratio. For instance, sample 1.5(12) is the geopolymer sample with Si/Al ratio of 1.5 and H<sub>2</sub>O/Na<sub>2</sub>O molar ratio of 12.

ATR-FTIR spectra were collected using a Varian FTS 7000 FT-IR spectrometer, with a Specac MKII Golden Gate single reflectance diamond ATR attachment with KRS-5 lenses and heater top plate. Absorbance spectra were collected from 4000-400 cm<sup>-1</sup> at a resolution of 2 cm<sup>-1</sup> and a scanning speed of 5 kHz with 32 scans. Scanning electron microscopy was also performed, using a Philips XL30 Field Emission Gun Scanning Electron Microscope (FEG-SEM). Fractured specimens were mounted on stubs and gold coated before analysis.

All geopolymer pastes were cured at 40°C in an oven. X-ray diffraction (XRD) (Phillips PW-1800) was conducted using CuK $\alpha$  X-rays, 30mA and 40 kV with 0.02° 2 $\theta$  steps, 2s step<sup>-1</sup>. Attenuated total reflectance Fourier-transform infrared (ATR-FTIR) spectroscopy was also used.

## 3. RESULTS AND DISCUSSION

The results presented in Figure 1 show the XRD diffractograms obtained for cured pastes after two weeks. The main crystalline phases identified in high water sample are quartz (SiO<sub>2</sub>, minor contaminant in amorphous geothermal silica) and faujasite (approximately Na<sub>2</sub>Al<sub>2</sub>Si<sub>3.3</sub>O<sub>10.6</sub>·7H<sub>2</sub>O), and in the sample with lower water content new peaks can be observed which are attributed to Zeolite A (approximately Na<sub>2</sub>Al<sub>2</sub>Si<sub>1.85</sub>O<sub>7.7</sub>·5.1H<sub>2</sub>O). The hump from 20 to 40° 2 $\theta$  in both samples demonstrates that a significant amount of the synthesized materials is X-ray amorphous, consistent with the majority of the geopolymers literature. The sharpness of the peaks in the lower-water sample may also be an indication of larger crystals.

It is of interest to note that the sample with less water added contained a greater extent of crystallite formation – this is contrary to many reports of reduced crystallinity with water addition to ‘traditional’ geopolymer systems, and suggests that there are additional effects occurring in the ‘one-part mix’ system that are not observed during silicate or hydroxide activation of aluminosilicate materials.

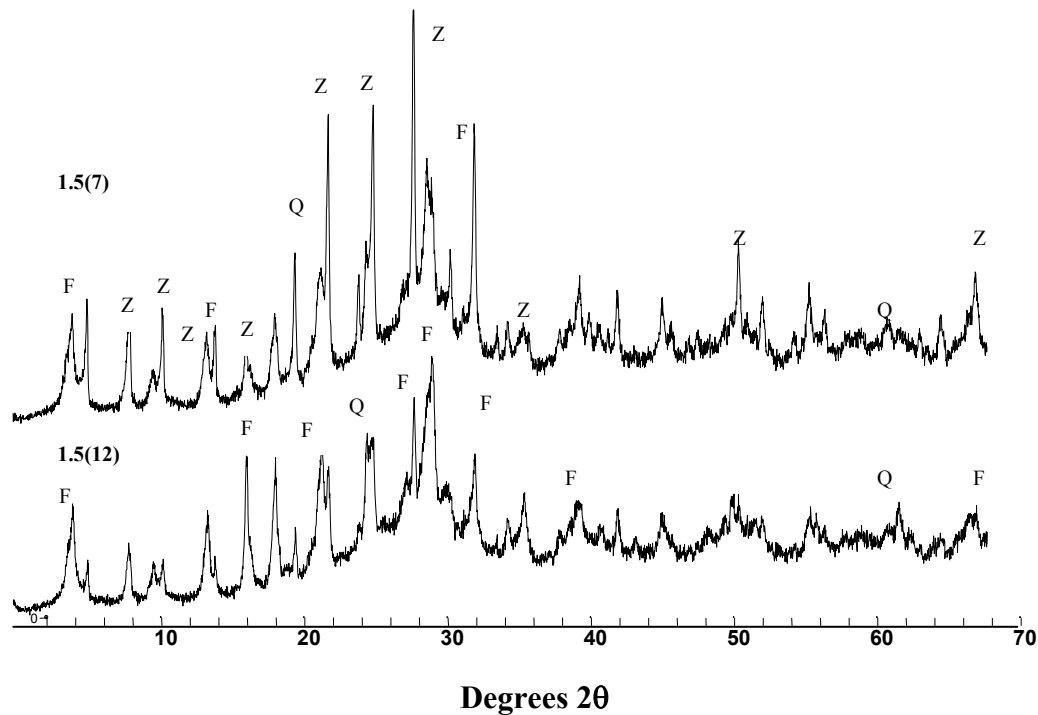


**Figure 1. XRD diffractograms of geopolymers derived from geothermal silica and sodium aluminate cured for two weeks. Prefixes refer to  $H_2O/Na_2O$  molar ratio. Q = quartz, F = faujasite, Z= zeolite A. Data from reference [7].**

Although XRD is an analytical technique commonly used for investigation of the geopolymer systems, it is important to note that this technique has significant limitations due to the apparent amorphicity of these materials[8]. So, other analytical techniques are required to provide insight about the structural characteristics of these materials, as well as the kinetics of structural evolution following mixing of the reactants.

The structural evolution of the geopolymer samples was therefore studied using ATR-FTIR (Figure 2). The spectra of geopolymer pastes for two samples are shown, as a function of reaction time over a 15-day period. Bands at  $1060\text{ cm}^{-1}$  are assigned to stretching of Si-O-Si bands at the surface of the unreacted silica particles [9], and bands at  $800$  and  $475\text{ cm}^{-1}$  relate to bending and rocking of the Si-O-Si bonds in the network of the unreacted geothermal silica [10]. Bands at  $625\text{ cm}^{-1}$  are related to the Al-O vibrations in the unreacted solid aluminate and bands at approximately  $700\text{ cm}^{-1}$  are assigned to  $AlO_3$  vibrations and a band at about  $545\text{ cm}^{-1}$  is related to a single Al-O-Al mode in the aluminate [11].

The position of the main Si-O-T stretching band gives an indication of the length and angle of the Si-O bands in the silicate network, and for amorphous silica this peak occurs at approximately  $1100\text{ cm}^{-1}$ [12]. This region is attributed to stretching vibration of inner  $SiO_2$  groups [9].

In the present work, main Si-O-T stretching band occurs at  $1060\text{ cm}^{-1}$  indicating the stretching vibrations of surface  $SiO_2$  groups[9]. Over time, main band shifts to lower wavenumbers in both samples that can be the indication of some probable changes in silicate network including an increase of non bridging oxygen in silicate sites, charge balancing by sodium cations in the system [13]or increasing the substitution of tetrahedral Al in the silicate network [14].

Over time, there is a reduction in intensity of the main Si-O-Si band indicating that the solid

silica is dissolving and changing in molecular structure. At the same time, a new band starts forming at about  $950\text{cm}^{-1}$  and the intensity of this band increases over time. This particular band is associated with the stretching vibrations of the Si-O-T (T: Si or Al) bond of the geopolymer network. The intensity of this band continues increasing gradually over time until there is only one clear band at  $940\text{ cm}^{-1}$  for both samples. The shoulder in  $1060\text{ cm}^{-1}$  is attributed to unreacted geothermal silica remaining in the samples.

Water plays a critical role during the dissolution, polycondensation and hardening stages of geopolymerization. Figure 2 shows that the dissolution of geothermal silica and the formation of geopolymer network bonds are much faster in the sample with lower water content.

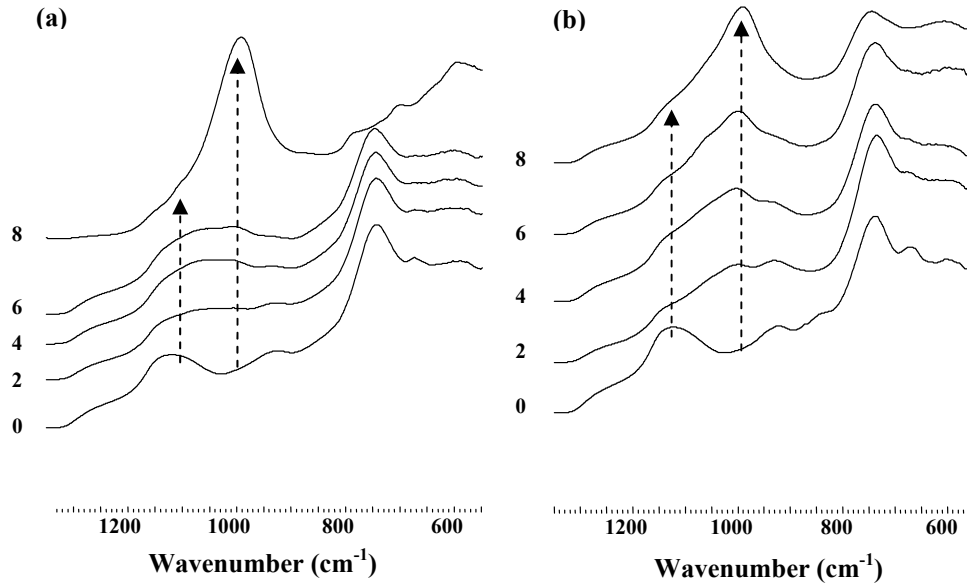


**Figure 2. ATR-FTIR spectra for geopolymer samples 1.5(12) (plot A) and 1.5(7) (plot B), showing the process of synthesis from geothermal silica and sodium aluminate. Numbers refer to the geopolymer age in days. Data from reference [7].**

Figure 3 shows the structural evolution of one-part mix geopolymer samples with different Si/Al ratios and the same amount of water. It is clear from these spectra that dissolution of geothermal silica and formation of geopolymer are faster in the sample with the lower Si/Al ratio

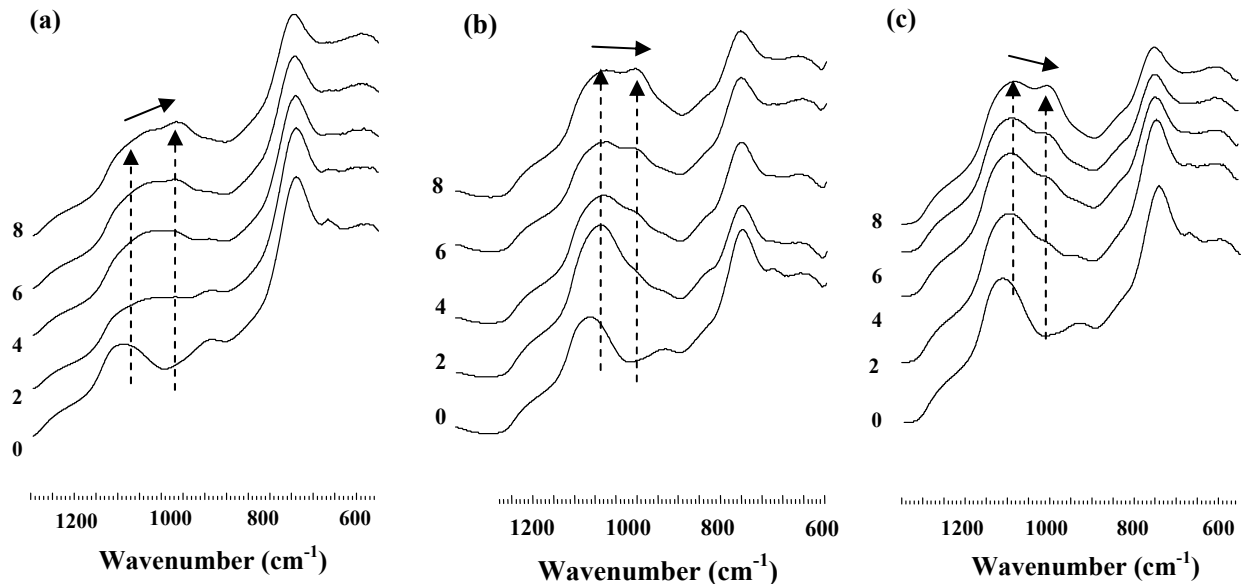


**Fig 3. ATR-FTIR spectra of (a) 1.5(12), (b) 2(12) and (c) 2.5(12) geopolymer samples. Numbers refer to the geopolymer age in days. Data from reference [7].**

These results show that the process of development of the geopolymer gel in the ‘just add water’ system studied here is relatively similar to the gel formation process in fly ash geopolymerization as was previously studied by this technique.[15-18] Both systems, although chemically very different, show the gradual destruction of the solid aluminate and silicate sources (which is very rapid in the case of solid sodium aluminate), and the formation of a new aluminosilicate gel phase characterized by a strong Si-O-T asymmetric stretching peak.

The durability of a cement structure strongly depends on its physical properties, such as permeability and ionic diffusivity, which are controlled by the microstructural characteristics of cement paste.[19] The porosity and pore size distribution are vital components of the microstructure of cement paste. The pore structure determines the permeability of cement, and thus the extent of penetration by aggressive agents.[20]

In order to study the microstructure of ‘just add water’-synthesized geopolymers, scanning electron microscopy (SEM) is used. Examples of the microstructures of sodium aluminate-geothermal silica geopolymers after two weeks are shown in Figure 4. An obvious difference can be observed between the two samples with different water contents. These micrographs show the greater extent of large pores, as well as larger size and higher density of gel particulates, in the sample with higher water content. Fine pore structure enables a material to better resist chemical attack as it leads to lower permeability.[21] Resistance to chloride penetration of mortar and concrete is one of the most important issues regarding the durability of concrete structures.[21-23]

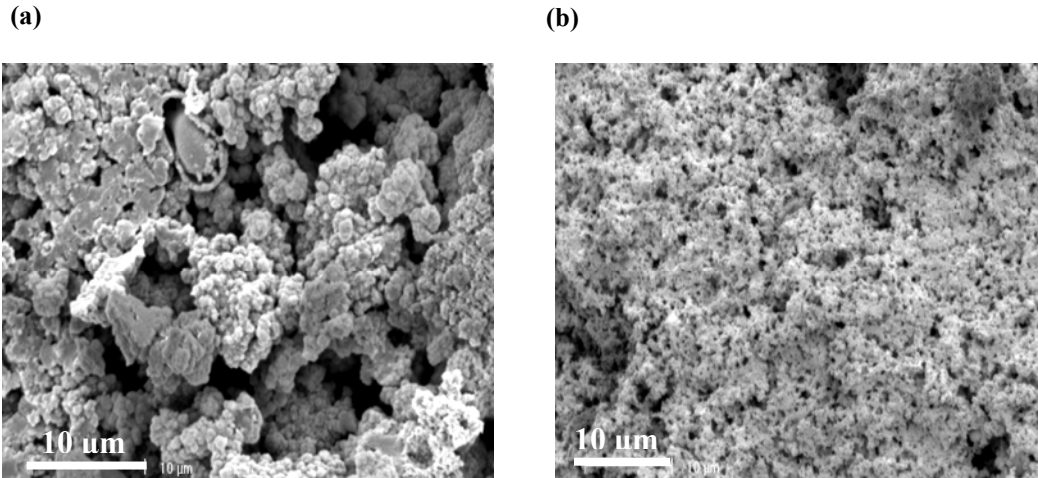


**Fig 4. SEM micrographs of (a) 1.5(12) and (b) 1.5(7) geopolymer samples after curing for two weeks at 40°C. Data from reference [7].**

In order to study the effect of Si/Al ratio on the microstructure of one part mix geopolymers, 2(12) and 2.5(12) samples were made using geothermal silica and sodium alumina, and their microstructures were also studied after two weeks' curing at 40°C (Figure 10). In traditional two-part geopolymer systems, the microstructure changes from containing large pores to being more homogenous with small pores as the Si/Al ratio increases.[24] Comparison of Figure 4 with Figure 5 shows the same behavior in the one-part system.

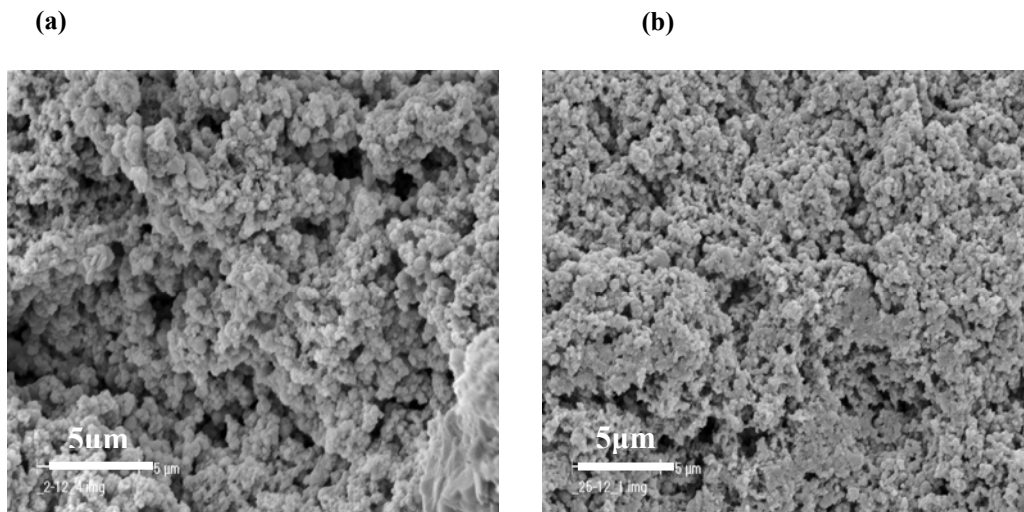


**Fig 5. SEM micrographs of (a) 2(12) and (b) 2,5(12) geopolymer samples after curing for two weeks at 40°C. Data from reference [7].**

## 4. CONCLUSIONS

The development of a solid replacement for the silicate activator in geopolymer synthesis will increase the commercial viability of this material by removing the difficulties associated with the use of viscous alkaline solutions. Also, the use of siliceous industrial wastes as silicate replacements in geopolymer cements for the construction industry can create an economical and environmentally friendly replacement for Portland cement, and finally a one-part mix or 'bag' of geopolymer cement can be made.

In this work, synthesis of a one part mix geopolymer from solid sodium aluminate and geothermal silica was investigated. This system demonstrates that making geopolymers from solid sources by "just adding water" is possible. Water plays a critical role during geopolymerization. Samples with less water have a greater extent of crystallite formation, which was unexpected because this is contrary to many reports of reduced crystallinity with water addition to 'traditional' geopolymer system. This difference may be due to the rapid dissolution of the aluminate source and relatively slower dissolution of silica source in the early stages of geopolymerisation. SEM micrographs clearly show the difference between samples with different water content and different Si/Al ratio. ATR-FTIR enables structural analysis of geopolymer samples during the geopolymerisation reaction.

## 5. ACKNOWLEDGMENTS

The assistance and guidance of Dr. Catherine Rees in this project is gratefully acknowledged. This work was funded in part through the Particulate Fluids Processing Centre (PFPC) (a Special Research Centre of the Australian Research Council), and by the Geopolymer Alliance.

## 6. References

1. J.L. Provis and J.S.J. van Deventer, *Geopolymerisation kinetics. 2. Reaction kinetic modelling*. Chemical Engineering Science, 2007, 62: p. 2318 - 2329.
2. W.K.W. Lee and J.S.J. van Deventer, *Use of infrared spectroscopy to study geopolymerization of heterogeneous amorphous aluminosilicates*. Langmuir, 2003, 19(21): p. 8726-8734.
3. M. Rowles and B. O'Connor, *Chemical optimization of the compressive strength of aluminosilicate geopolymers synthesized by sodium silicate activation of metakaolinite*. Journal of Materials Chemistry, 2003(13): p. 1161-1165.
4. J.M. Rincon, *Thermal behaviour of silica waste from a geothermal power station and derived silica ceramics*. Journal of Thermal Analysis and Calorimetry, 1999, 56(1): p. 1261-1269.
5. C. Diaz and F.J. Valle-Fuentes, *Use of silicon residue in ceramics and glass*. American Ceramic Society Bulletin, 1999, 78(8): p. 112-115.
6. C. Rees, *Mechanisms and Kinetics of Gel Formation in Geopolymers*, Ph.D. Thesis, University of Melbourne, 2007
7. A. Hajimohammadi, J.L. Provis, and J.S.J. van Deventer, *One-part geopolymer mixes from geothermal silica and sodium aluminate*. Industrial & Engineering Chemistry Research, 2008: p. In press.

8. P.A. Jacobs, E.G. Derouane, and J. Weitkamp, *Evidence for X-ray-amorphous zeolites*. Journal of the Chemical Society, Chemical Communications, 1981: p. 591 - 593.
9. J. Osswald and K.T. Fehr, *FTIR spectroscopic study on liquid silica solutions and nanoscale particle size determination*. Journal of Material Science 2006, 41: p. 1335-1339.
10. R.J. Bell and P. Dean, *Atomic vibrations in vitreous silica*. Discussions of the Faraday Society, 1970, 50: p. 55-61.
11. R.J. Moolenaar, J.C. Evans, and L.D. McKeever, *The structure of the aluminate ion in solutions at high pH*. Journal of Physical Chemistry, 1970, 74(20): p. 3629-3638.
12. M. Handke and W. Mozgawa, *Vibrational spectroscopy of the amorphous silicates*. Vibrational Spectroscopy, 1993, 5(1): p. 75-84.
13. J.R. Sweet and W.B. White, *Study of sodium silicate glasses and liquids by infrared reflectance spectroscopy*. Physics and Chemistry of Glasses, 1969, 10(6): p. 246-251.
14. B.N. Roy, *Infrared spectroscopy of lead and alkaline-earth aluminosilicate glasses*. Journal of the American Ceramic Society, 1990, 73(4): p. 846-855.
15. C.A. Rees, J.L. Provis, G.C. Lukey, and J.S.J. van Deventer, *Attenuated total reflectance fourier transform infrared analysis of fly ash geopolymer gel aging*. Langmuir, 2007, 23: p. 8170-8179.
16. C.A. Rees, J.L. Provis, G.C. Lukey, and J.S.J. van Deventer, *In situ ATR-FTIR study of the early stages of fly ash geopolymer gel formation*. Langmuir, 2007, 23: p. 9076-9082.
17. A. Fernández-Jiménez, A.G. de la Torre, A. Palomo, G. Lopez-Olmo, M.M. Alonso, and M.A.G. Aranda, *Quantitative determination of phases in the alkali activation of fly ash. Part I. Potential ash reactivity*. Fuel, 2006, 85(5-6): p. 625-634.
18. A. Fernández-Jiménez, A.G. de la Torre, A. Palomo, G. López-Olmo, M.M. Alonso, and M.A.G. Aranda, *Quantitative determination of phases in the alkaline activation of fly ash. Part II: Degree of reaction*. Fuel, 2006, 85(14-15): p. 1960-1969.
19. P. Chindapasirt, C. Jaturapitakkul, and T. Sinsiri, *Effect of fly ash fineness on compressive strength and pore size of blended cement paste*. Cement & Concrete Composites, 2005, 27: p. 425-428.
20. P. Chindapasirt, S. Homwuttiwong, and V. Sirivivatnanon, *Influence of fly ash fineness on strength, drying shrinkage and sulfate resistance of blended cement mortar*. Cement and Concrete Research, 2004 34: p. 1087-1092.
21. P. Chindapasirt, S. Rukzon, and V. Sirivivatnanon, *Resistance to chloride penetration of blended Portland cement mortar containing palm oil fuel ash, rice husk ash and fly ash*. Construction and Building Materials, 2008 22: p. 932-938.
22. M.D.A. Thomas, P.B. Bamforth, and F.T. Bingham, *Modelling chloride diffusion in concrete. Effect of fly ash and slag*. Cement and Concrete Research, 1999, 29: p. 487-495.



23. C.S. Poon, Y.L. Wong, and L. Lam, *The influence of different curing conditions on the pore structure and related properties of fly-ash cement pastes and mortars*. *Construction and Building Materials*, 1997, 11: p. 383-393.
24. P. Duxson, J.L. Provis, G.C. Lukey, S.W. Mallicoat, W.M. Kriven, and J.S.J. van Deventer, *Understanding the relationship between geopolymer composition, microstructure and mechanical properties*. *Colloids and Surfaces A: Physicochemical and Engineering Aspects*, 2005, 269(1-3): p. 47-58.